Original Research

Evaluation of a bilayered, micropatterned hydrogel dressing for full-thickness wound healing

Chelsea M Magin[1], Dylan B Neale[2], Michael C Drinker[1], Bradley J Willenberg[2,3,4], Shravanthi T Reddy[1], Krista MD La Perle[5], Gregory S Schultz[2] and Anthony B Brennan[1,4,7]

[1]Sharklet Technologies, Inc., Aurora, CO 80045, USA; [2]Department of Materials Science and Engineering, University of Florida, Gainesville, FL 32611, USA; [3]Department of Internal Medicine, University of Central Florida, Orlando, FL 32827, USA; [4]Saisijin Biotech, LLC, Orlando, FL 32827, USA; [5]Department of Veterinary Biosciences, College of Veterinary Medicine and Comparative Pathology & Mouse Phenotyping Shared Resource, Comprehensive Cancer Center The Ohio State University, Columbus, OH 43210, USA; [6]Department of Obstetrics and Gynecology and Institute for Wound Research, University of Florida, Gainesville, FL 32610, USA; [7]J. Crayton Pruitt Family Department of Biomedical Engineering, University of Florida, Gainesville, FL 32611, USA
Corresponding author: Chelsea M Magin. Email: cmagin@sharklet.com

Abstract

Nearly 12 million wounds are treated in emergency departments throughout the United States every year. The limitations of current treatments for complex, full-thickness wounds are the driving force for the development of new wound treatment devices that result in faster healing of both dermal and epidermal tissue. Here, a bilayered, biodegradable hydrogel dressing that uses microarchitecture to guide two key steps in the proliferative phase of wound healing, re-epithelialization, and revascularization, was evaluated *in vitro* in a cell migration assay and *in vivo* in a bipedicle ischemic rat wound model. Results indicate that the Sharklet™-micropatterned apical layer of the dressing increased artificial wound coverage by up to 64%, $P = 0.024$ *in vitro. In vivo* evaluation demonstrated that the bilayered dressing construction enhanced overall healing outcomes significantly compared to untreated wounds and that these outcomes were not significantly different from a leading clinically available wound dressing. Collectively, these results demonstrate high potential for this new dressing to effectively accelerate wound healing.

Keywords: Micropattern, wound healing, biomaterials, hydrogel, gelatin, microarchitecture

***Experimental Biology and Medicine* 2016; 241: 986–995. DOI: 10.1177/1535370216640943**

Introduction

Wounds are a significant cause of morbidity and impaired quality of life affecting approximately 8.6 million patients in the U.S. annually.[1] The most costly and debilitating wounds—e.g. severe burns, traumatic lacerations, or non-healing/chronic wounds—are often deep, complex, and require reconstruction using autologous skin grafts.[2,3] Although autologous skin grafting is the current ''gold standard'' treatment, it is not without serious limitations. Potential complications include risk of infection,[4] graft necrosis,[2,5] excessive pain at the donor site,[6,7] and discoloration and scarring.[5] Failure of graft/donor site healing is often due to underlying physiological conditions, including age[8] and comorbidities such as diabetes or circulatory conditions.[9] As our population ages and the incidence of chronic diseases increases, the occurrence of costly delayed skin graft healing will rise accordingly. Therefore, it is imperative to develop advanced full-thickness dressings that provide an alternative to skin grafting for both traumatic and chronic wounds.

Injuries result in loss of skin structure to varying degrees, and therefore, the requirements for replacing lost skin greatly depend on the type and extent of the wound. Superficial wounds result in loss of the outermost layer of the skin—the epidermis. This layer maintains the barrier function of the skin and consists of epithelial cells called keratinocytes at increasing stages of differentiation.[10,11] In more serious injuries, the loss of the epidermal layer and part or all of the dermis (i.e. a partial or full-thickness wound, respectively) results in the need to replace or reconstruct two vital tissue types to restore skin integrity. The dermis is responsible for the mechanical properties of skin due to its composition mainly of fibroblasts and their associated extracellular matrix (ECM).[11] Collagen is the most abundant protein in the dermal ECM representing 25%–35% of the whole-body protein content.[12] Research has shown that contact with collagen and collagen-derived fragments in wound dressings controls many cellular functions.[12] In fact, modified collagen wound dressings have been shown to induce a more robust transient inflammatory

response, improve vascularization, and increase collagen deposition in preclinical swine models of full-thickness excisional wounds[13] and chronic wounds.[14]

In addition to the biochemical cues provided to cells when binding to natural hydrogel materials such as collagen or collagen fragments, both the tissue structure of the dermal basal lamina and the organization of fibrillar collagen within the ECM guide fibroblast and epithelial cell migration, respectively, from the wound margins.[15] In fact, the dermal/epidermal junction in native skin is not flat but consists of a series of micro-scale ridges and projections.[16] These physical cues modulate keratinocyte maturation, differentiation, and function, and in turn are essential for tissue organization and integrity of skin structure. These underlying principles can be leveraged synthetically to achieve similar outcomes more efficiently—e.g. simple channels 150 μm deep and 50 μm wide enhanced re-epithelialization rates and resulted in tissue structure similar to that achieved by the same cells cultured on acellular dermis.[17] Likewise, microgrooves 1 μm and 5 μm deep with groove spacing from 1 μm to 10 μm enhanced and directed migration of individual epithelial cells and cells from intact epithelial tissue.[18] These results showed that microtopographies direct migration of cells regardless of whether the physical cues present at a wound margin are biotic or abiotic.

The orientation and elongation of cells in response to the physical properties of the underlying substratum is known as contact guidance.[19] This phenomenon is a key regulator of angiogenesis—new blood vessel formation[20,21]—and cellular migration.[22,23] The bilayered, full-thickness wound dressing evaluated here harnesses the capacity of physical guidance cues to accelerate vascularization of the wound bed as well as coverage of the wound surface. The first layer consists of Capgel™, an alginate-based material that forms regularly ordered, tunable anisotropic capillaries through self-assembly[24,25] and serves as a dermal template. The 3D-microarchitecture that forms within Capgel has been shown to support blood vessel infiltration in a rat myocardial infarction model.[26] It has also been shown that dermal revascularization after full-thickness wounding proceeds via ingrowth of vessels from the wound edges through previously formed channels.[21] We thus hypothesize that the Capgel foundation will promote neovascularization and granulation tissue formation.

The dermal foundation created by the Capgel technology will accelerate epidermal healing on the apical Sharklet™-micropatterned surface of the wound dressing. Coverage of a wound by keratinocytes or re-epithelialization is viewed as a hallmark of successful wound healing.[27] Re-epithelialization by proliferation and migration of keratinocytes starts within 72 h of injury and continues for approximately 14 days. During the proliferation healing stage, cell migration is a critical element of the healing process. The Sharklet micropattern uses contact guidance at the apical layer to actively orient the direction and speed of migration to predictably accelerate wound closure.[27] Systematic studies on Sharklet micropatterns have related topographic feature geometry and surface chemistry to biological adhesion,[28–30] cellular morphology,[31,32] and migration in specific, predictable ways. In this way, subtle alterations in the micropattern attributes based on the algorithms associated with the technology can be used to achieve a predictable cellular response. Optimization of the Sharklet micropattern to achieve early re-epithelialization has the potential to not only reduce risk of infection and lower patient pain but to also initiate the remodeling of underlying granulation tissue, which reduces the possibility of hypertrophic scarring.[27]

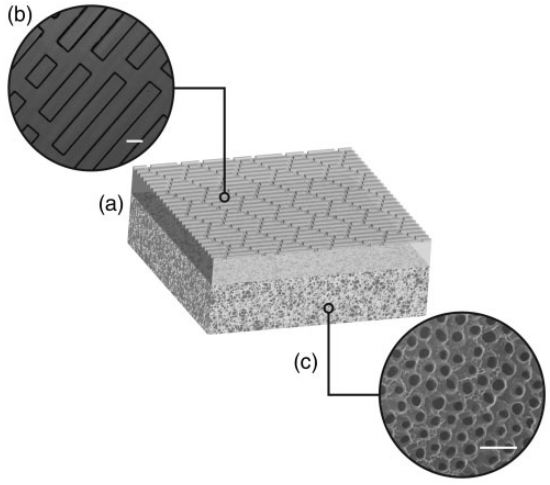

Figure 1 Schematic of the bilayered wound dressing. (a) 3D representation of the dressing construction including a Sharklet-patterned apical layer and the Capgel dermal microchannels. (b) Confocal microscopy image of the Sharklet-patterned apical layer. (c) Scanning electron microscopy image of the Capgel dermal microchannels reproduced by permission of Taylor & Francis http://www.tandfonline.com).[35] Scale bars, 50 μm

Therefore, we hypothesized that wound dressings comprise gelatin (denatured collagen) with engineered microarchitectures such as the Sharklet micropattern and the Capgel 3D microchannels (Figure 1) would enhance the wound-healing environment by guiding apical cell proliferation and migration to achieve rapid epidermal wound closure, while also guiding cellular invasion and capillary growth within the underlying dermis.[11] Here, we investigate the potential for engineered microarchitectures to enhance full-thickness wound healing both *in vitro* and *in vivo* in a bipedicle, ischemic rat skin flap model.[33,34]

Materials and methods

Sample fabrication

Sharklet micropatterns were designed on two size scales (e.g. 5-μm and 50-μm spacings) (Table 1) based on previously reported results, which demonstrated that channels of these sizes enhanced re-epithelialization and recapitulated the texture of the native epidermal–dermal junction.[17,36] Various aspect ratios (i.e. ratio of topography height to topography width) were tested to optimize micropattern height for guiding cell migration. Briefly, new Sharklet micropatterns were designed, digitized, and printed to a photomask. Photolithographic techniques were used to transfer the pattern on the photomask to a photoresist-coated silicon wafer. Next, the patterned silicon wafer was etched to a desired depth using deep reactive ion etching. The processed silicon wafer served as a template

for creating molds for topographical replication.[37] A platinum-catalyzed polydimethylsiloxane elastomer (PDMSe) (Xiameter® RTV-4232-T2, Dow Corning Corporation) was cast on silicon wafer templates to form negative micropatterned molds. Sharklet-micropatterned gelatin hydrogels were formed using filter-sterilized components in standard cell culture conditions by self-assembly on PDMSe molds with or without Sharklet micropatterns. A solution of gelatin (6% w/v in deionized water; Sigma), warmed 37°C to facilitate dissolution, was pipetted onto PDMSe templates. The solution-filled molds were cooled to 4°C for 1 h to solidify the gelatin. Next, hydrogels were chemically crosslinked with a solution of 0.119 M 1-ethyl-3-(3-dimethylaminopropyl) carbodiimide hydrochloride (EDC) (Sigma) and 0.113 M N-Hydroxysuccinimide (NHS) (Fisher) in phosphate buffered saline (PBS) (pH 7.4, Gibco, Life Technologies) at 4°C for 18 h.[38] Crosslinked gelatin films were subsequently trimmed to form 20-mm discs and covalently attached to an amine-functionalized glass coverslip for ease of handling in cell culture assays. Micropatterned gelatin hydrogels were evaluated for pattern transfer and pattern fidelity using confocal microscopy (Olympus LEXT OLS 4000). Feature height, width, and spacing were measured and compared to the dimensions of the original mold using the software package that comes with the LEXT OLS 4000.

Human epidermal keratinocyte migration assay

A modified scratch assay was used to model cellular migration during wound healing *in vitro*.[22,39] Sharklet micropatterned and smooth gelatin hydrogels backed to coverslips were swollen in PBS storage solution (i.e. PBS containing 1 mg/mL amphotericin B and 50 U/mL penicillin) for at least 24 h prior to the start of each assay. Samples were oriented so that the long edges of the topographic features were parallel to the wound (Figure 2(a)). Rectangular (3 mm × 20 mm) PDMSe patches were placed along the center of each sample (Figure 2(a)). Primary adult human epidermal keratinocytes (HEKs) were labeled with a cytoplasmic dye (CellTracker Green CMFDA [5-Chloromethylfluorescein Diacetate], Life Technologies, Carlsbad, CA) to facilitate live cell imaging without affecting cell viability or function[40] and subsequently seeded onto test surfaces at an initial density of 6000 cells/cm^2 (Figure 2(b)). HEKs were cultured in growth media (ATCC Dermal Cell Basal Medium containing 0.4% bovine pituitary extract, 0.5 ng/mL rh TGA-α, 3 mM L-Glutamine, 100 ng/mL hydrocortisone, 5 μg/mL insulin, 1 μg/mL epinephrine, and 5 μg/mL apo-trasferrin) at 37°C and 5% CO_2. Upon reaching approximately 70% confluence, the PDMSe patches were removed (Figure 2(c)) to allow cell migration across the wound surface.

Cell migration was monitored with live cell fluorescent imaging, using an Olympus BX63 fluorescent microscope every 2 days after patch removal. To quantify migration, samples were fixed with 4% paraformaldehyde (Electron Microscopy Sciences, Hatfield, PA) at room temperature for 15 min, mounted using ProLong® Gold Antifade Reagent (Life Technologies, Carlsbad, CA) and imaged across the wounded area. The area covered by cells within the wounded area was measured, and the average percent area coverage was calculated for each sample type at the assay endpoint (day 4) using ImageJ Software (National Institutes of Health [NIH], Bethesda, MD).[22]

Table 1 Dimensions of Sharklet-micropatterns tested

Surface	Height (μm)	Width (μm)	Spacing (μm)	Aspect ratio
+1SK10 × 5	1	10	5	0.1
+10SK50 × 50	10	50	50	0.2

Prototype design and production

The top-performing Sharklet micropattern (+10SK50 × 50) from the HEK migration assay was scaled up to the appropriate size for a wound dressing and tested in an established delayed-healing model in rats to validate healing behavior for a broad range of non-healing/chronic wounds.[33,34,41] The apical layers of the wound-dressing prototypes were produced following the same procedure outlined above to make gelatin hydrogels. Then the solution-filled molds were cooled to 4°C for 1 h to solidify the

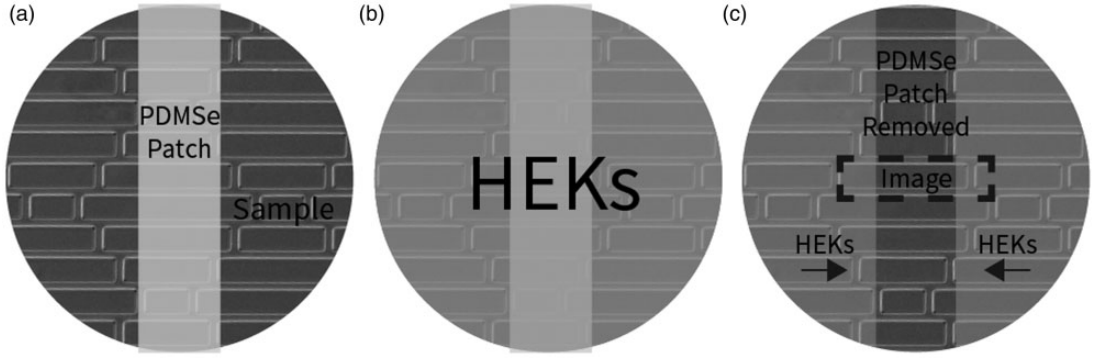

Figure 2 Schematic of the HEK migration assay procedure. (a) Samples were arranged with the features oriented parallel to the direction of cell migration and a rectangular PDMSe patch was placed across each sample to block cell adhesion. (b) Cells were seeded onto the entire surface and allowed to grow to approximately 70% confluence. (c) PDMSe patches were removed and cell migration into the artificial wound was monitored

gelatin. Next, 2 mL of Capgel slurry was synthesized as previously described[24,25] and packed into a PDMSe mold ($d = 20$ mm) on top of the solid gelatin. The apical gelatin layer and the basement Capgel layers were chemically crosslinked with a solution of 0.6 M EDC and 0.2 M NHS in PBS at 4°C for 18 h.[24,38] The silicone mold was removed from the construct, and a 6-mm biopsy punch was used to create appropriately sized dressings. The dressings were then washed in PBS for 1 h and followed by three changes of 10 × saline sodium citrate (SSC) (20 × SSC, Fisher BioReagants, diluted with deionized water to 10×) over the course of 24 h. Finally, dressings were washed with three changes of normal saline over the course of 24 h and subsequently sterilized by soaking in Minncare Sterilant (3% solution in deionized water) (Mar Cor, Plymouth MN) for 10 min prior to a final PBS rinse and implantation.

Ischemic wound model

All animal experiments were conducted under a protocol approved by the University of Florida Animal Care and Use Committee and in compliance with the standards in the ''Guide for Care and Use of Laboratory Animals'' published by the NIH. After appropriate anesthetization, the dorsal aspect of 20 male Sprague-Dawley rats weighing ~250–300 g were shaved, and a rectangular template was centered on the spine between the base of the scapula and the iliac crest. The template was used to outline the placement of four circular holes and the placement of vertical tissue-flap incisions. Four full-thickness wounds were created at the corresponding markings using a 6-mm biopsy punch. These normal skin punches were fixed in 10% neutral buffered formalin for subsequent analysis. To create a condition of transient ischemia, two parallel linear incisions were cut along the sides of the template. The skin flap created was elevated to sever the underlying vasculature, repositioned, and stapled on each lateral side.[33,34] One of each of the four dressings: (1) the novel bilayer Sharklet-micropatterned apical layer with the combined Capgel neovascularization technology, (2) a smooth apical layer with Capgel, (3) Endoform, a dermal template that is currently in clinical use as a commercial competitor, and (4) no treatment. The Endoform dermal template consists of a naturally derived ovine collagen ECM.[42] All wounds were covered with a compressible secondary dressing and covered with Vetrap (3 M).

On post-surgery days 7, 10, and 14, rats ($n = 6$) were euthanized.[33,34] Two rats were also euthanized on post-surgery day 28 to qualitatively observe the extent of dressing degradation. Tissue biopsies were collected using 8-mm biopsy punches, fixed in 10% neutral buffered formalin, embedded in paraffin, sectioned and stained with either hematoxylin and eosin (H&E) or Masson's Trichrome. Histological wound sections were evaluated by a veterinary pathologist, board certified by the American College of Veterinary Pathologists, for dressing location, re-epithelialization, acute and chronic inflammation, granulation tissue formation and neovascularization using an established, semi-quantitative histologic scoring scale (Table 2).[43,44] Results were analyzed to assess clinically relevant outcomes of each treatment that enhance the wound-healing environment—e.g. epithelial coverage, vascularization, and overall wound healing, a composite score including all measured outcomes.

Statistical analysis

Area coverage measurements (A) were normalized via logarithmic transformation for migration assays. Log increases were calculated for each experiment by subtracting the average log (A_{smooth}) from the average log

Table 2 Quantitative wound-healing histologic scoring system.[43,44]

	Score			
Variable	**0**	**1**	**2**	**3**
Dressing	None noted	Majority/all noted under epidermis or within dermis	Majority/all noted superficially or above dermis	N/A
Re-epithelialization	None; significant epidermal defect	Partial, incomplete, discontinuous	Complete with epidermis of normal thickness	Complete but hyperplastic epidermis
Acute inflammation (presence of neutrophils)	None	Scant	Moderate	Abundant
Chronic inflammation (presence of lymphocytes, plasma cells, macrophages)	None	Scant	Moderate	Abundant
Granulation tissue	None	Scant; partial across wound gap or depth; immature, loose	Moderate; partial across wound gap or depth; immature, loose	Abundant; complete across wound gap and entire depth; mature, dense
Neovascularization	None	Up to 5 vessels per high-powered field of view (40 × magnification)	6 to 10 vessels per high-powered field of view (40 × magnification)	Greater than 10 vessels per high-powered field of view (40 × magnification)

($A_{micropattern}$). Normality of each data set was confirmed by residual and normal probability plots. The mean log increase was converted to the median percent increase using the equation: $1–10^{LI}$.

Statistically significant increases from three experiments (*in vitro*) were compared with the null hypothesis of zero increase by a one-sided test of the difference in means. Estimates of the among- and within-experiment variances were assessed using analysis of variance (ANOVA) of the log transformed area coverage values for each smooth and micropatterned sample, with random effect for experiment (*in vitro*). The average histologic score ($n = 6$ replicates, *in vivo*) for each condition was assessed using ANOVA and *post hoc* Tukey Test for multiple comparisons. All analyses were performed using MiniTab16 statistical software (State College, PA).

Results

Sample fabrication

When micropatterning hydrogels, highly hydrated crosslinked polymer networks such as gelatin, it is important to control swelling in order to precisely pattern features. Here, micropatterning and crosslinking steps were performed using highly hydrated gelatin solutions to reduce the impact of water uptake on final feature dimensions. Following crosslinking and swelling in PBS, confocal images of the surfaces were taken, and feature dimensions were measured. Measurements confirmed patterns transferred with feature dimensions, including height, width, and spacing within the tolerances defined by the original silicon wafer molds (Figure 3).

HEK migration assay

Quantification revealed that both Sharklet-micropatterns, oriented parallel to the direction of cell migration, significantly increased the area of artificial wound coverage compared to the smooth standard after 4 days. The smaller pattern (+1SK10 × 5) increased coverage by 46%, $P = 0.045$ and the larger pattern (+10SK50 × 50) increased coverage by 64%, $P = 0.024$ (Figure 4) relative to the smooth standard. The best performing pattern (+10SK50 × 50) was selected for prototype production and testing *in vivo* in an ischemic wound model.

Ischemic wound model

Qualitative assessment of representative photomicrographs of H&E stained sections of rat skin 7 days post-wounding (Figure 5) show indications of improved healing outcomes

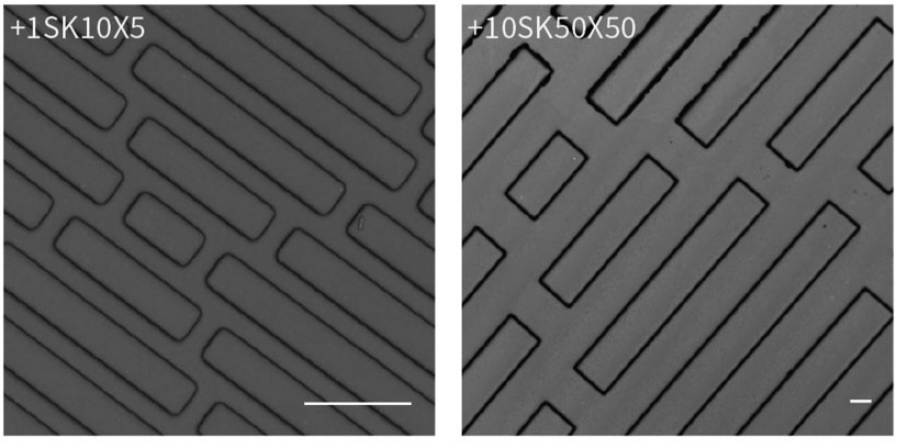

Micropattern	Feature Dimension	Wafer Dimension	Measured in Gelatin
+1SK10x5	Height	1.0 ± 0.5 μm	1.1 ± 0.1 μm
	Width	10 ± 1 μm	9.1 ± 0.4 μm
	Spacing	5 ± 1 μm	4.8 ± 0.4 μm
+10SK50x50	Height	10 ± 1 μm	9.8 ± 0.6 μm
	Width	50 ± 5 μm	49 ± 2 μm
	Spacing	50 ± 5 μm	46 ± 2 μm

Figure 3 Representative confocal images of the two new Sharklet micropatterns replicated in gelatin. Measurements reported as mean ± SD confirm pattern transfer within the tolerances defined by the wafer dimensions, which are reported as target ± tolerance. Scale bars, 25 μm

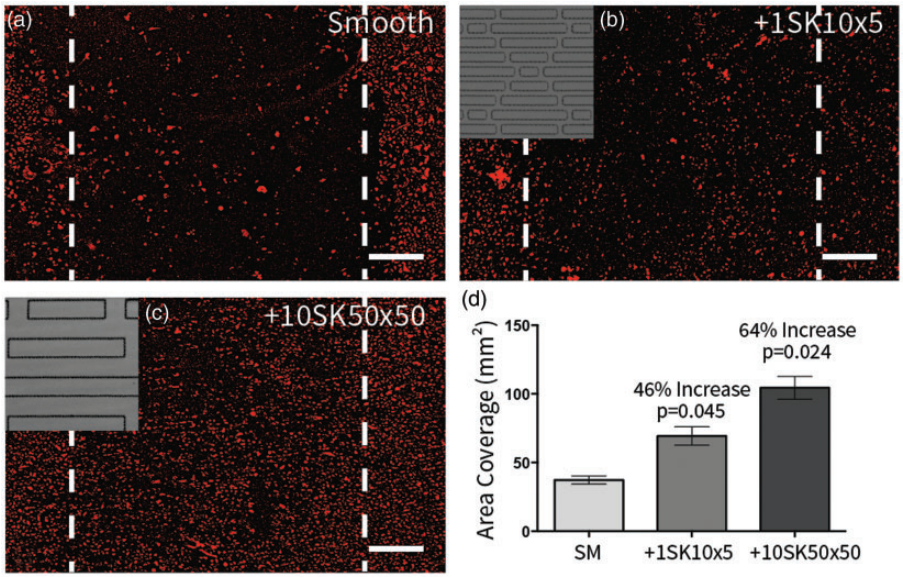

Figure 4 Representative fluorescent microscopy images of HEKs (red) on (a) smooth, (b) + 1SK10 × 5, and (c) + 10SK50 × 50 gelatin surfaces. Sharklet-micropatterns, oriented parallel to the direction of cell migration, increased the area coverage of artificial wounds (marked by dashed lines) compared to the smooth standard after 4 d. The best performing pattern (+10SK50 × 50) increased coverage (d) by 64%, $P = 0.024$ relative to a smooth standard. Scale bars, 500 μm

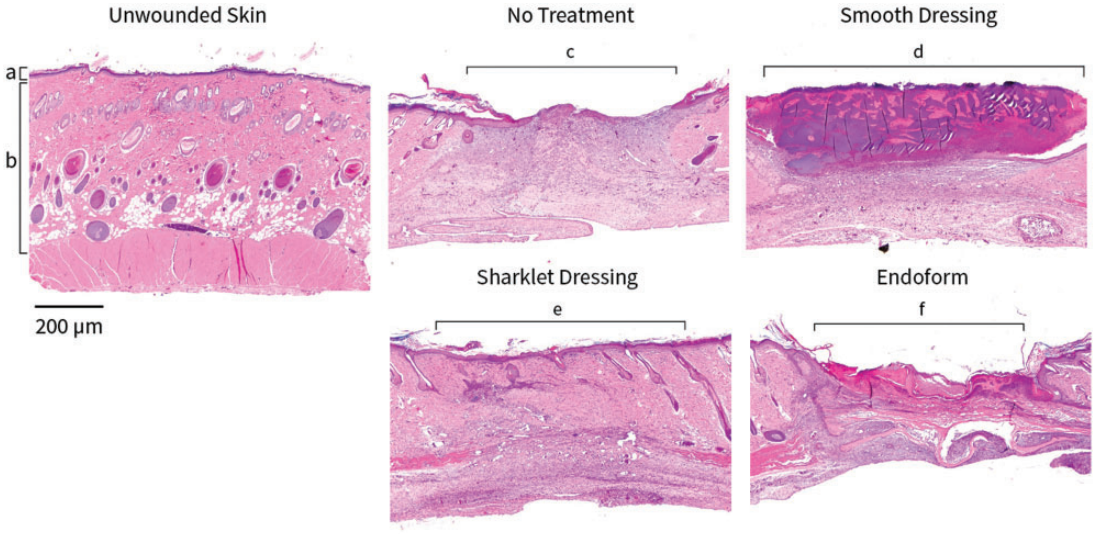

Figure 5 Representative photomicrographs of H&E stained sections of rat skin 7 d post-wounding. (a) The structure of the epidermis in unwounded, control rat skin. (b) The structure of the dermis in unwounded, control rat skin. (c) Indicates the wounded area on the no treatment group. These wounds exhibit higher levels of contraction, incomplete epithelial coverage, and differences in dermal structure compared to native skin. (d) Denotes the wounded area on skin treated with the Smooth dressing. In this image, the dressing is not completely incorporated below the epidermis (Score 2), epithelialization is incomplete, and the structure of the dermis is not consistent with unwounded skin. (e) Shows the wounded area on skin treated with the Sharklet dressing. These wounds exhibit complete re-epithelialization, reduced contracture compared to no treatment or Endoform-treated wounds, and a dermal structure that more closely mimics natural skin. (f) Indicates the wounded area treated with Endoform, a clinically available dermal template dressing. Wounds treated with Endoform demonstrate higher levels of contraction than those dressed with the bilayered constructs, incomplete epithelialization, and reduced amounts and maturation of granulation tissue formation on day 7

for wounds treated with bilayered dressings compared to untreated controls. Untreated wounds, in general, exhibited higher levels of contraction, incomplete re-epithelialization, and differences in dermal structure compared to unwounded skin (Figure 5(c)). Both bilayered dressing constructs showed more complete re-epithelialization, reduced contracture compared to untreated or Endoform-treated wounds, and dermal regeneration that more closely mimics natural skin (Figure 5(d) and (e)). Wounds treated with Endoform, a clinically available dermal template dressing, exhibited higher levels of contraction than those dressed with the bilayered constructs, incomplete epithelialization, and reduced amount and maturity of granulation tissue formation on day 7 (Figure 5(f)).

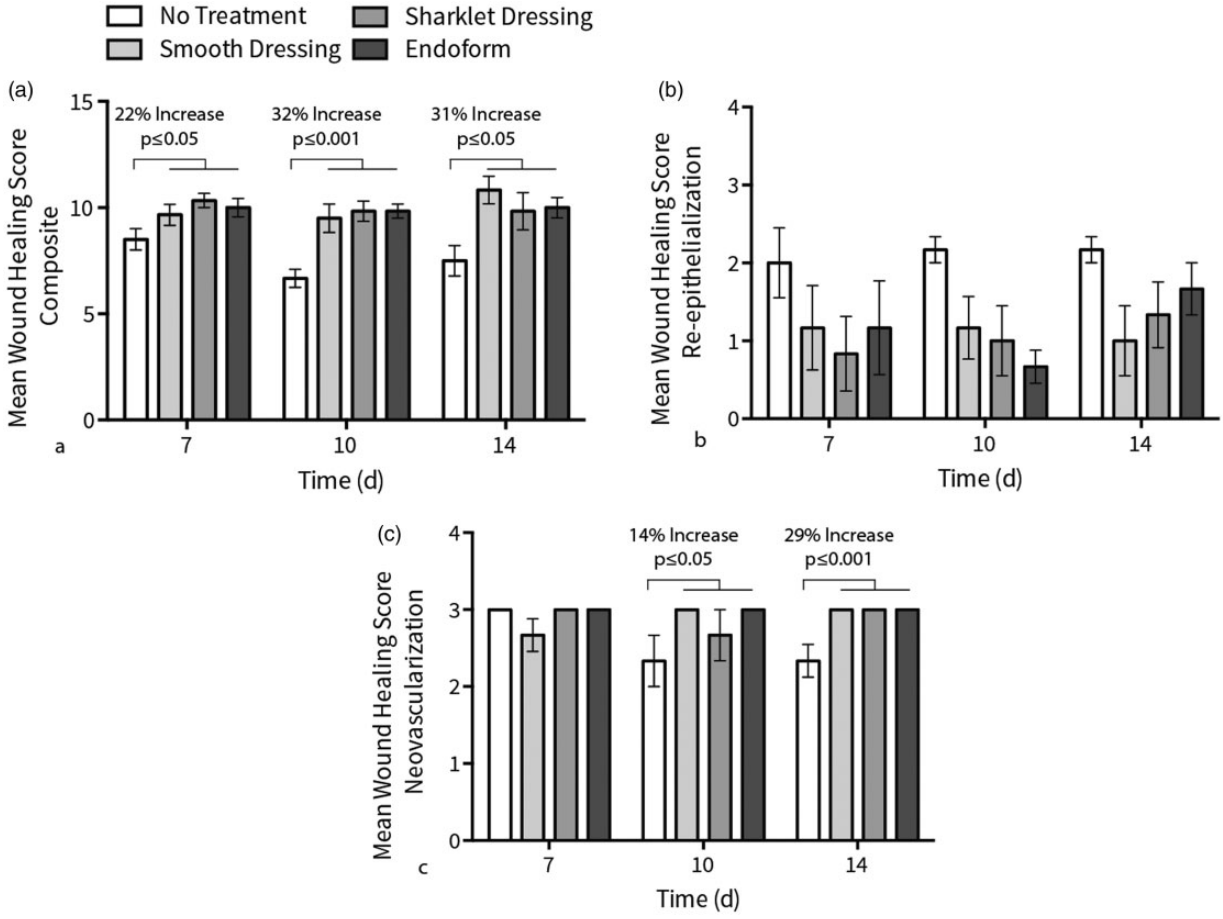

Figure 6 Histologic wound-healing scores. (a) Mean overall wound-healing score composite including grading for dressing location, re-epithelialization, acute and chronic inflammation, granulation tissue formation, and neovascularization. All dressing types showed significantly improved healing versus no treatment. Statistically significant increases over no treatment are reported for all dressings, which were not significantly different among groups. (b) Mean re-epithelialization scores indicate no significant differences among treatment groups. (c) Mean neovascularization results show higher numbers of new blood vessels formed in wounds treated with dressings versus no treatment but no significant differences among dressing types. Overall improved healing versus no treatment and outcomes comparable to a standard care treatment, i.e. the Endoform dermal template, demonstrate potential for the bilayered wound dressing constructs to improve healing outcomes

Semi-quantitative wound-healing scores from histologic grading reveal that bilayered constructs improve overall healing compared to untreated wounds, and these improvements are not statistically different from those measured on Endoform-treated wounds (Figure 6(a)). Composite wound-healing scores include evaluation of dressing location, re-epithelialization, acute and chronic inflammation, granulation tissue formation, and neovascularization. All dressings, smooth, Sharklet-patterned, and Endoform exhibited increases in composite mean wound-healing scores compared to no treatment at 7 (22% increase, $P \leq 0.05$), 10 (32% increase, $P \leq 0.001$) and 14 (31% increase, $P \leq 0.05$) days post-wounding. Evaluation of re-epithelialization showed no significant differences among groups (Figure 6(b)). The average wound-healing scores for neovascularization demonstrated increases for all treatment groups over the no treatment negative controls but no significant differences among treatment groups. The dressings resulted in more blood vessels per field of high powered view ($40\times$ magnification) over untreated controls at 10 (14%, $P \leq 0.05$) and 14 (29%, $P \leq 0.001$) days post-wounding (Figure 6(c)). Qualitative observations ($n = 2$) of H&E stained sections of rat skin 28 days post-wounding demonstrated that the bilayered, hydrogel dressings degraded *in vivo* over this period of time (Figure 1 in Supplementary Material).

Discussion

All major categories of wound dressings exhibit significant limitations when applied to full-thickness wounds, which truly require treatment for both layers of skin.[45] Despite many advances in our understanding of wound healing,[45–49] the treatment of full-thickness wounds has focused primarily on regenerating dermis,[50,51] while neglecting or even impeding re-epithelialization of the epidermal layer. No clinically available dressings have all of the characteristics required to repair the dermis and epidermis concurrently.[52] While synthetic skin grafts (e.g. Endoform™, Biobrane®, and Integra®) are used to enhance dermal healing,[51] these products can take up to three weeks to vascularize, allowing for complications to occur during

that extended timeframe.[53] These products also do not directly promote re-epithelialization. Biobrane® and Integra®, for instance, include a silicone-based top layer that must be removed after dermal regeneration to allow epidermal healing.[52] The need to remove this top dressing layer is a key drawback of many synthetic wound dressings. It disrupts epithelial cell migration and new tissue formation, and it increases costs and patient discomfort.[54] In an international survey of wound-care specialists, nearly 60% said that they would prefer a one-piece composite for burn treatment to reduce frequency of dressing changes.[54]

Natural hydrogels are promising materials for regeneration of both dermis and epidermis due to their high water content, inherent biocompatibility, recognition by endogenous cells, and biodegradability.[55] Many ECM-mimicking materials derived from natural polymers have been investigated in both *in vitro* and *in vivo* preclinical models for wound-healing applications. Zhao et al.[56] developed photocrosslinkable gelatin (i.e. gelatin methacrylamide) with tunable properties and demonstrated that these hydrogels supported keratinocyte growth, differentiation, and stratification into reconstructed multilayered epidermis with barrier function *in vitro*. Porous gelatin scaffolds fabricated through freeze-drying,[57] cryogelation,[58] or salt-leaching[59] methods have all been evaluated for wound-healing applications. These scaffolds all supported cellular in-growth and viability in benchtop studies. When evaluated *in vivo* in a full-thickness murine model, however, porous gelatin scaffolds enhanced dermal healing but did not improve re-epithelialization—a limitation also observed on clinically available wound treatment devices.[57,59]

The bilayered wound dressing evaluated here is a novel technology designed to complement these strategies and potentially overcome the limitations of full-thickness wound healing using engineered physical guidance cues, including (1) a dermal template with 3D microarchitecture to accelerate neovascularization, and (2) Sharklet micropatterning on the apical layer of the dressing to encourage autologous epidermal healing via guided cell migration. Confocal imaging demonstrated that chemically crosslinking a highly hydrated gelatin solution using EDC and NHS resulted in high fidelity transfer of micropatterned features from silicone molds (Figure 3). All feature dimensions including height, width, and spacing were measured to be within the±10% tolerances defined by the original silicon wafer mold. This fabrication technique facilitated the production and testing of micropatterned gelatin surfaces both *in vitro* and *in vivo*.

The dermal–epidermal junction in native skin consists of a series of epidermal rete ridges and dermal papillary projections ranging from 50 to 400 μm in width and from 50 to 200 μm in depth, which serve as both a microscopic 3D cellular microenvironment[60] and a macroscopic structural support for the skin tissue.[16] The results of this study demonstrate that Sharklet micropatterns created on a similar size scale (+10SK50 × 50) increased migration rates of HEKs by up to 64%, $P = 0.024$ (Figure 4) compared to smooth surfaces made of the same material. Cell infiltration during wound healing primarily occurs through migration of cells from the wound margins[11] and has been identified as the rate-limiting step in the wound closure process.[61] Micropatterned substrates guide cell polarization and migration by influencing the spatial arrangement, establishment and maturation of focal adhesions.[62] This mechanism has been validated with many different cell types including epithelial cells[18,63,64] and fibroblasts,[65] the two cell types primarily responsible for wound repair. In addition to taking advantage of this contact guidance principle to accelerate epidermal healing, the bilayered wound dressing evaluated here provides a template for cellular growth patterns that mimic the natural architecture of the dermal–epidermal junction. This 3D cellular microenvironment modulates keratinocyte functions through coordination of cell–cell and cell–matrix interactions. Pins et al. developed microfabricated dermal–epidermal regeneration matrices comprised of 50 μm wide channels and showed that these synthetic 3D microenvironments may indeed create a protective environment for a regenerative population of keratinocytes similar to that of native skin tissue.[17,60] Based on these findings, the advantage of the Sharklet-micropatterned apical layer on the bilayered dressing evaluated here may be twofold: (1) accelerated epidermal cell migration and (2) guided development of appropriate keratinocyte niches at the dermal–epidermal junction.

In fact, *in vivo* assay results revealed that the bilayered wound dressing structure significantly improved composite wound healing and revascularization scores compared to untreated controls. Additionally, these scores were not statistically different from those obtained in wounds treated with a clinically available dermal template, Endoform (Figure 6). Although, it was hypothesized that the Sharklet-micropatterned apical layer would accelerate re-epithelialization, no quantitative differences among treatment groups were measured (Figure 6(b)). This outcome could be due in part to a limitation of the rodent wound-healing model. Small mammals such as rats have several anatomical and physiological characteristics that differ substantially from human skin. Most importantly, their wounds close primarily through contraction as opposed to re-epithelialization as noted in humans.[66] Due to significant contracture, it was not possible to directly compare the Sharklet-patterned apical layer to other treatment options for enhanced re-epithelialization in this model. Qualitatively significant contracture was observed in untreated and Endoform-treated wounds. For this reason, it is likely that both composite wound-healing scores and re-epithelialization grades could improve in a model that more closely mimics healing in human skin. The improvements measured in this model provide a foundation for studies to validate enhanced wound-healing outcomes, including re-epithelialization, in particular, in a porcine model; wound-healing studies in pigs show a remarkable 78% concordance with human study results.[66]

Conclusion

Collectively, these results indicate high potential that a full-thickness, woundcare dressing that exploits cellular responses to microarchitectural cues may enhance the proliferative phase of wound healing, i.e. promote both

neovascularization and re-epithelialization. Follow-on preclinical trials in a porcine model will demonstrate the potential of this novel dressing to reduce treatment cost and patient suffering while minimizing scarring and wound instability.

Author contributions: CMM designed *in vitro* experiments, managed animal experiment collaborations, performed all data analysis, and wrote the manuscript; DBN synthesized composite dressings and performed animal experiments; MCD assisted with experimental design and performed *in vitro* experiments; BJW helped develop the synthesis of the composite dressing and provided experimental design input for animal experiments; STR provided advice on project scope; GSS provided animal experiment expertise and input for *in vivo* experimental design; KMDL performed the histopathologic analysis of rodent wounds, including the selection and modification of the scoring scheme, evaluation and histologic and photomicrographic documentation; and ABB provided material science expertise. All authors edited the final manuscript.

ACKNOWLEDGEMENTS

The authors thank B. C. Stevenson for imaging and characterizing micropatterned samples and M. R. Mettetal for producing Figure 1. This work was supported by grant funding from the National Institute of Arthritis, Musculoskeletal and Skin Diseases SBIR Phase I Grant Number: 1R43AR067584, and supported in part by grant P30 CA16058, National Cancer Institute, Bethesda, MD.

DECLARATION OF CONFLICTING INTERESTS

The author(s) declared the following potential conflicts of interest with respect to the research, authorship, and/or publication of this article: CMM, MCD, STR and ABB are all employees of Sharklet Technologies, Inc.

REFERENCES

1. Ambulatory and Hospital Care Statistics, Centers for Disease Control. National Hospital Ambulatory Medical Care Survey: 2010 Emergency Department Summary Tables. Available at: http://www.cdc.gov/nchs/data/ahcd/nhamcs_emergency/2010_ed_web_tables.pdf (2010, accessed 22 March 2016).
2. Johnson TM, Ratner D, Nelson BR. Soft tissue reconstruction with skin grafting. *J Am Acad Dermatol* 1992;**27**:151
3. McGregor AD. *Free skin grafts, Fundamental Techniques of Plastic Surgery*, 10th ed. London: Churchill Livingstone, 2000, pp. 35–59
4. Ünal S, Ersoz G, Demirkan F, Arslan E, Tütüncü N, Sari A. Analysis of skin-graft loss due to infection: infection-related graft loss. *Ann Plast Sur* 2005;**55**:102
5. Branham GH. *Facial soft tissue reconstruction*. Shelton, CT: PMPH-USA, 2011
6. Demirtas Y, Yagmur C, Soylemez F, Ozturk N, Demir A. Management of split-thickness skin graft donor site: a prospective clinical trial for comparison of five different dressing materials. *Burns* 2010;**36**:999
7. Orlik J, Horwich P, Bartlett C, Trites J, Hart R, Taylor S. Long-term functional donor site morbidity of the free radial forearm flap in head and neck cancer survivors. *J Otolaryngol* 2014;**43**:1
8. Sgonc R, Gruber J. Age-related aspects of cutaneous wound healing: A mini-review. *Gerontology* 2013;**59**:159
9. Boateng JS, Matthews KH, Stevens HNE, Eccleston GM. Wound healing dressings and drug delivery systems: a review. *J Pharmaceut Sci* 2008;**97**:2892
10. Moghaddam AS, Kamolz LP, Weninger W, Parvizi D, Wiedner M, Lumenta DB. The use of Keratinocytes: Things we should keep in mind! *Eur Surg* 2013;**45**:154
11. Singer AJ, Clark RAF. Cutaneous wound healing. *New Engl J Med* 1999;**341**:738
12. Brett DA. Review of collagen and collagen-based wound dressings. *Wounds* 2008;**20**:347–56
13. Elgharably H, Roy S, Khanna S, Abas M, DasGhatak P, Das A, Mohammed K, Sen CK. A modified collagen gel enhances healing outcome in a preclinical swine model of excisional wounds. *Wound Repair Regen* 2013;**21**:473
14. Elgharably H, Ganesh K, Dickerson J, Khanna S, Abas M, Ghatak PD, Dixit S, Bergdall V, Roy S, Sen CK. A modified collagen gel dressing promotes angiogenesis in a preclinical swine model of chronic ischemic wounds. *Wound Repair Regen* 2014;**22**:720
15. Krawczyk WS. A pattern of epidermal cell migration during wound healing. *J Cell Biol* 1971;**49**:247
16. Odland GF. The morphology of the attachment between the dermis and the epidermis. *Anat Rec* 1950;**108**:399
17. Bush KA, Pins GD. Development of microfabricated dermal epidermal regenerative matrices to evaluate the role of cellular microenvironments on epidermal morphogenesis. *Tissue Eng* 2012;**18**:2343
18. Dalton BA, Walboomers XF, Dziegielewski M, Evans MDM, Taylor S, Jansen JA, Steele JG. Modulation of epithelial tissue and cell migration by microgrooves. *J Biomed Mater Res* 2001;**56**:195
19. Harrison R. The reaction of embryonic cells to solid structures. *J Exp Zool* 1914;**17**:521
20. Uttayarat P, Toworfe GK, Dietrich F, Lelkes PI, Composto RJ. Topographic guidance of endothelial cells on silicone surfaces with micro- to nanogrooves: Orientation of actin filaments and focal adhesions. *J Biomed Mater Res Part A* 2005;**75A**:668
21. Capla JM, Ceradini DJ, Tepper OM, Callaghan MJ, Bhatt KA, Galiano RD, Levine JP, Gurtner GC. Skin graft vascularization involves precisely regulated regression and replacement of endothelial cells through both angiogenesis and vasculogenesis. *Plast Reconstr Surg* 2006;**117**:836
22. Marmaras A, Lendenmann T, Civenni G, Franco D, Poulikakos D, Kurtcuoglu V, Ferrari A. Topography-mediated apical guidance in epidermal wound healing. *Soft Matter* 2012;**8**:6922
23. Moon JJ, Hahn M, Kim I, Nsiah B, West JL. Micropatterning of poly(ethylene glycol) diacrylate hydrogels with biomolecules to regulate and guide endothelial morphogenesis. *Tissue Eng* 2009;**15**:579
24. Willenberg BJ, Zheng T, Meng F-W, Meneses JC, Rossignol C, Batich CD, Terada N, Steindler DA, Weiss MD. Gelatinized coppercapillary alginate gel functions as an injectable tissue scaffolding system for stem cell transplants. *J Biomater Sci Polymer Ed* 2011;**22**:1621
25. Della Rocca DG, Willenberg BJ, Ferreira LF, Wate PS, Petersen JW, Handberg EM, Zheng T, Steindler DA, Terada N, Batich CD, Byrne BJ, Pepine CJ. A degradable, bioactive, gelatinized alginate hydrogel to improve stem cell/growth factor delivery and facilitate healing after myocardial infarction. *Med Hypotheses* 2012;**79**:673
26. Rocca DGD, Willenberg BJ, Franklin LF, Porvasnik SL, Petersen JW, Wate PS, Handberg EM, Schultz G, Romeo F, Batich CD, Byrne BJ, Pepine CJ. An injectable acellular capillary hydrogel improves left ventricular function after myocardial infarction. *J Am Coll Cardiol* 2012;**59**:E856
27. Stefonek TJ, Masters KS. Immobilized gradients of epidermal growth factor promote accelerated and directed keratinocyte migration. *Wound Repair Regen* 2007;**15**:847
28. Decker JT, Kirschner CM, Long CJ, Finlay JA, Callow ME, Callow JA, Brennan AB. Engineered antifouling microtopographies: an energetic model that predicts cell attachment. *Langmuir* 2013;**29**:13023–30
29. Magin CM, Finlay JA, Clay G, Callow ME, Callow JA, Brennan AB. Antifouling performance of cross-linked hydrogels: refinement of an attachment model. *Biomacromolecules* 2011;**12**:915

30. Schumacher JF, Carman ML, Estes TG, Feinberg AW, Wilson LH, Callow ME, Callow JA, Finlay JA, Brennan AB. Engineered antifouling microtopographies – effect of feature size, geometry, and roughness on settlement of zoospores of the green alga. *Ulva Biofouling* 2007;**23**:55
31. Magin C. *Engineered microtopographies and surface chemistries direct cell attachment and function*. Gainesville, FL: University of Florida, 2010
32. Carman ML. Engineered microtopographies to induce *in vitro* endothelial cell morphologies stable to shear. *Biomedical engineering*. Gainesville, FL: University of Florida, 2007
33. Chen C, Schultz GS, Bloch M, Edwards PD, Tebes S, Mast BA. Molecular and mechanistic validation of delayed healing rat wounds as a model for human chronic wounds. *Wound Repair Regen* 1999;**7**:486
34. Gowda SM, Weinstein DA, Blalock TD, Gandhi K, Mast BA, Chin G, Schultz GS. Topical application of recombinant platelet-derived growth factor increases the rate of healing and the level of proteins that regulate this response. *International Wound Journal* 2013;**12**:564–71
35. Willenberg BJ, Hamazaki T, Meng F-W, Terada N, Batich C. Self-assembled copper-capillary alginate gel scaffolds with oligochitosan support embryonic stem cell growth. *J Biomed Mater Res Part A* 2006;**79A**:440
36. Bush KA, Downing BR, Walsh SE, Pins GD. Conjugation of extracellular matrix proteins to basal lamina analogs enhances keratinocyte attachment. *J Biomed Mater Res Part A* 2007;**80A**:444
37. Carman ML, Estes TG, Feinberg AW, Schumacher JF, Wilkerson W, Wilson LH, Callow ME, Callow JA, Brennan AB. Engineered antifouling microtopographies – correlating wettability with cell attachment. *Biofouling* 2006;**22**:11
38. Kuijpers AJ, Engbers GHM, Krijgsveld J, Zaat SAJ, Dankert J, Feijen J. Cross-linking and characterisation of gelatin matrices for biomedical applications. *J Biomater Sci Polymer Ed* 2000;**11**:225
39. Magin CM, May RM, Drinker MC, Cuevas KH, Brennan AB, Reddy ST. Micropatterned protective membranes inhibit lens epithelial cell migration in posterior capsule opacification model. *Transl Vis Sci Techol* 2015;**4**:1
40. Kirschner CM, Anseth KS. In situ control of cell substrate microtopographies using photolabile hydrogels. *Small* 2013;**9**:578
41. Brown GL, Nanney LB, Griffen J, Cramer AB, Yancey JM, Curtsinger LJ, Holtzin L, Schultz GS, Jurkiewicz MJ, Lynch JB. Enhancement of wound healing by topical treatment with epidermal growth factor. *New Engl J Med* 1989;**321**:76
42. Lun S, Irvine SM, Johnson KD, Fisher NJ, Floden EW, Negron L, Dempsey SG, McLaughlin RJ, Vasudevamurthy M, Ward BR, May BCH. A functional extracellular matrix biomaterial derived from ovine forestomach. *Biomaterials* 2010;**31**:4517
43. Abramov Y, Golden B, Sullivan M, Botros SM, Miller J-JR, Alshahrour A, Goldberg RP, Sand PK. Histologic characterization of vaginal vs. abdominal surgical wound healing in a rabbit model. *Wound Repair Regen* 2007;**15**:80
44. Braiman-Wiksman L, Solomonik I, Spira R, Tennenbaum T. Novel insights into wound healing sequence of events. *Toxicol Pathol* 2007;**35**:767
45. Singh MR, Saraf S, Vyas A, Jain V, Singh D. Innovative approaches in wound healing: trajectory and advances. *Artif Cells Nanomed Biotechnol* 2013;**41**:202
46. Reinke JM, Sorg H. Wound repair and regeneration. *Eur Surg Res* 2012;**49**:35
47. Ovington LG. Advances in wound dressings. *Clin Dermatol* 2007;**25**:33
48. Moura LIF, Dias AMA, Carvalho E, de Sousa HC. Recent advances on the development of wound dressings for diabetic foot ulcer treatment—a review. *Acta Biomater* 2013;**9**:7093
49. Martin C, Low WL, Amin MCIM, Radecka I, Raj P, Kenward K. Current trends in the development of wound dressings, biomaterials and devices. *Pharmaceut Patent Anal* 2013;**2**:341
50. Heitland A, Piatkowski A, Noah EM, Pallua N. Update on the use of collagen/glycosaminoglycate skin substitute–six years of experiences with artificial skin in 15 German burn centers. *Burns* 2004;**30**:471
51. Moiemen N, Yarrow J, Hodgson E, Constantinides J, Chipp E, Oakley H, Shale E, Freeth M. Long-term clinical and histological analysis of Integra dermal regeneration template. *Plast Reconstr Surg* 2011;**127**:1149
52. Halim A, Shah J, Khoo T. Biologic and synthetic skin substitutes: an overview. *Indian J Plast Surg* 2010;**43**:23
53. Téot L, Otman S, Trial C, Brancati A. The use of noncellularized artificial dermis in the prevention of scar contracture and hypertrophy. *Wound Repair Regen* 2011;**19**:s49
54. Selig HF, Lumenta DB, Giretzlehner M, Jeschke MG, Upton D, Kamolz LP. The properties of an ''ideal'' burn wound dressing – what do we need in daily clinical practice? Results of a worldwide online survey among burn care specialists. *Burns* 2012;**38**:960
55. Van Vlierberghe S, Dubruel P, Schacht E. Biopolymer-based hydrogels as scaffolds for tissue engineering applications: a review. *Biomacromolecules* 2011;**12**:1387
56. Zhao X, Lang Q, Yildirimer L, Lin ZY, Cui W, Annabi N, Ng KW, Dokmeci MR, Ghaemmaghami AM, Khademhosseini A. Photocrosslinkable gelatin hydrogel for epidermal tissue engineering. *Adv Healthc Mater* 2016;**5**:108–18
57. Choi YS, Lee SB, Hong SR, Lee YM, Song KW, Park MH. Studies on gelatin-based sponges. Part III: A comparative study of cross-linked gelatin/alginate, gelatin/hyaluronate and chitosan/hyaluronate sponges and their application as a wound dressing in full-thickness skin defect of rat. *J Mater Sci Mater Med* 2001;**12**:67
58. Dainiak MB, Allan IU, Savina IN, Cornelio L, James ES, James SL, Mikhalovsky SV, Jungvid H, Galaev IY. Gelatinfibrinogen cryogel dermal matrices for wound repair: preparation, optimisation and in vitro study. *Biomaterials* 2010;**31**:67
59. Lee SB, Kim YH, Chong MS, Hong SH, Lee YM. Study of gelatin-containing artificial skin V: fabrication of gelatin scaffolds using a salt-leaching method. *Biomaterials* 2005;**26**:1961
60. Clement AL, Moutinho TJ Jr, Pins GD. Micropatterned dermal-epidermal regeneration matrices create functional niches that enhance epidermal morphogenesis. *Acta Biomaterialia* 2013;**9**:9474
61. McClain SA, Simon M, Jones RA, Nandi A, Gailit JO, Tonnesen MG, Newman D, Clark RA. Mesenchymal cell activation is the rate-limiting step of granulation tissue induction. *Am J Pathol* 1996;**149**:1257
62. Huttenlocher A, Horwitz AR. Integrins in cell migration. *Cold Spring Harbor Perspect Biol* 2011;**3**:a005074
63. Karkhaneh A, Mirzadeh H, Ghaffariyeh A, Ebrahimi A, Honarpisheh N, Hosseinzadeh M, Heidari MH. Novel materials to enhance corneal epithelial cell migration on keratoprosthesis. *Br J Ophthalmol* 2011;**95**:405
64. Teixeira AI, Abrams GA, Bertics PJ, Murphy CJ, Nealey PF. Epithelial contact guidance on well-defined micro- and nanostructured substrates. *J Cell Sci* 2003;**116**:1881
65. Jeon H, Hidai H, Hwang DJ, Healy KE, Grigoropoulos CP. The effect of micronscale anisotropic cross patterns on fibroblast migration. *Biomaterials* 2010;**31**:4286
66. Roy S, Biswas S, Khanna S, Gordillo G, Bergdall V, Green J, Marsh CB, Gould LJ, Sen CK. Characterization of a preclinical model of chronic ischemic wound. *Physiol Genom* 2009;**37**:211